Article **Journal Civil Engineering**
December 2022, Vol.6 No.16 32-45

Hybrid nanocomposite of vanadium dioxide and carbon nanotubes embedded in a gypsum binder for thermal energy storage

Incorporación de un nanocompuesto híbrido de dióxido de vanadio con nanotubos de carbono en pastas de yeso para almacenamiento térmico

VILLEGAS-MENDEZ, Jesús Roberto†, FIGUEROA-TORRES, Mayra Zyzlila*, GUERRA-COSSÍO, Miguel Ángel and RUVALCABA-AYALA, Fabián René

Universidad Autónoma de Nuevo León, Facultad de Ingeniería Civil

ID 1st Author: *Jesús Roberto, Villegas-Méndez* / **ORC ID**: 0000-0001-9595-0823, **CVU CONACYT ID**: 1106862

ID 1st Co-author: *Mayra Zyzlila, Figueroa-Torres* / **ORC ID**: 0000-0002-6823-7384, **CVU CONACYT ID**: 42436

ID 2nd Co-author: *Miguel Ángel, Guerra-Cossío* / **ORC ID**: 0000-0003-0336-5112, **CVU CONACYT ID**: 558134

ID 3rd Co-author: *Fabián René, Ruvalcaba-Ayala* / **ORC ID**: 0000-0002-0519-6685, **CVU CONACYT ID**: 177937

DOI: 10.35429/JCE.2022.16.6.32.45 Received September 20, 2022; Accepted December 30, 2022

Abstract

This investigation studied the heat storage capacity of a gypsum blinder with a hybrid nanocomposite (NH) of vanadium dioxide and multiwall carbon nanotubes (VO_2/MWCNT). The influence of the NH in the hydration kinetics and hydrated products was determined. The effect of the incorporated amount of NH in the wettability, mass loss by humectation-drying cycles, thermal conductivity, specific heat (Cp) and gypsum thermal performance at 40 °C was determined. Characterization techniques exhibited that the presence of VO_2/MWCNT did not modify hydration kinetics and phases development, water drop angle or compressive strength. Nevertheless, gypsum blinders mass loss increased with the presence of the nanocomposite after 6 humectation-drying cycles. According to the thermal properties, it was found that the NH addition increased gypsum blinders thermal conductivity and Cp values. Finally, it was concluded that gypsum with VO_2/MWCNT promotes self-thermal regulation properties without affecting its performance. The usage of VO_2/MWCNT embedded in a gypsum as a construction material would provide thermal comfort conditions in buildings.

Heat, Comfort, Energy

Resumen

Esta investigación estudió la capacidad de almacenamiento de calor en una pasta de yeso al incorporar un nanocompuesto híbrido (NH) de dióxido de vanadio con nanotubos de carbono multiparedes (VO_2/MWCNT). Asimismo, se determinó la influencia del NH en la cinética de hidratación del yeso y las fases hidratadas. En función de la cantidad de NH adicionada, se realizó un seguimiento a la mojabilidad del yeso, la pérdida de masa por ciclos de humectación-secado, la resistencia a la compresión, conductividad térmica, calor específico (Cp) y desempeño térmico al exponer las muestras a 40 °C. Los resultados mostraron que la incorporación del VO_2/MWCNT en el yeso no modifica la cinética ni el desarrollo de los productos de hidratación, la mojabilidad o la resistencia a la compresión. Además, se encontró que la presencia del NH propicia la pérdida de masa después de 6 ciclos de humectación-secado. Adicionalmente, se determinó que la adición del VO_2/MWCNT incrementa la conductividad térmica y el Cp. Se concluyó que la integración del VO_2/MWCNT en el yeso favorece el desarrollo de propiedades térmicas de autorregulación de calor sin afectar su integridad por lo que, su uso como material de construcción favorecería el confort térmico al interior de una edificación.

Calor, Confort, Energía

Citation: VILLEGAS-MENDEZ, Jesús Roberto, FIGUEROA-TORRES, Mayra Zyzlila, GUERRA-COSSÍO, Miguel Ángel and RUVALCABA-AYALA, Fabián René. Hybrid nanocomposite of vanadium dioxide and carbon nanotubes embedded in a gypsum binder for thermal energy storage. Journal Civil Engineering. 2022. 6-16: 32-45

† Researcher contributing as first author.
* Author's Correspondence (e-mail: m.zyzlila@gmail.com)

Introduction

The development of mankind has led to an increase in the energy demand required to meet basic needs. By the end of 2021, global gross energy consumption will increase by 5.8 % (bp report, 2022). This is worrying because of the contribution to the carbon footprint caused by this increase. Despite the different actors responsible for global energy consumption, the building sector alone uses 40 % of the total gross energy produced (Amaral *et al.*, 2017). Furthermore, it is estimated that around 60% of energy consumption in a building is used by thermal regulation systems in order to provide thermal comfort inside (Faraj *et al*., 2020). From this problem arises the need to generate materials or methods to improve the thermal behaviour of buildings that promote a more efficient performance of thermal regulation systems (Faraj *et al*., 2020).

In this regard, the incorporation of phase change materials (PCMs) in conventional building materials (Alzoubi *et al*., 2020) such as gypsum has been studied because it is a commonly used material in construction due to its low energy cost of production (Lushnikova & Dvorkin, 2016) and its fire resistance (Castellón *et al*., 2021) and acoustic insulation (Boccarusso *et al*., 2020) properties.

PCMs are materials with the ability to store heat latently through a change of state (solid, liquid or gas), this modification occurs at a transition temperature (Tc) with a specific enthalpy called latent heat (Frazzica *et al*., 2019). The use of PCMs is intended to provide traditional building materials with the ability to store a fraction of the heat received in the open to decrease the amount of heat transferred to the interior of buildings (Jeong *et al*., 2019).

Despite the variety of PCMs available, studies on building materials have focused on the use of PCMs with a phase change from solid to liquid state because most of these have a Tc between 20 and 40 °C and a latent heat of 60 to 230 J/g, properties established as ideal for the application of these types of systems (Tyagi & Buddhi, 2007).

However, they show low compatibility with cementitious materials due to the low cohesion between their particles, with leakage of the PCM during the change of state, as well as a decrease in mechanical strength. Guardia *et al*. report a 50 % decrease in the compressive strength of white cement pastes incorporated with commercial paraffin at 20 % of the total weight of the mixtures (Guardia *et al*., 2019). Sic., Cunha *et al*. present a study on the decrease of up to 75% by adding commercial paraffin between 5 and 20% of the total weight of ordinary Portland cement pastes (Cunha *et al*., 2020). On the other hand, there are solid-solid PCMs with melting points between 30 and 68°C and latent heat between 10 and 150 J/g (Fallahi *et al*., 2017). Despite having a higher Tc with lower latent heat than liquid-liquid PCMs, solid-solid PCMs could offer better mechanical stability when mixed with cementitious materials, since they maintain their solid state during their transition, which would prevent PCM leakage and allow better cohesion between PCM particles and the cementitious material (Raj *et al*., 2020).

PCMs in general prove to be an excellent alternative for the development of innovative construction materials, although, most PCMs exhibit low thermal conductivity (λ) (Cheng *et al*., 2020). This characteristic is reflected in the heat storage-release dynamics, since, when interacting with ambient heat the PCM has greater difficulty in absorbing and/or releasing it (Zuo *et al*., 2020). This characteristic has been reduced by coupling materials with high thermal conductivity such as carbon-based materials into PCM (Coppola *et al*., 2016). In doing so, improvements in thermal conductivity of up to 200% have been obtained (Guardia *et al*., 2019; Kim *et al*., 2021). Yu *et al*. used a commercial vegetable oil-based PCM with a thermal conductivity of 0.199 W/mK, to which carbon nanotubes were incorporated at 5% of the total weight of the mixture, obtaining a thermal conductivity of 0.536 W/mK (Yu *et al*., 2014).

Based on the above, in this research, a NH of VO2/MWCTN was prepared as a solid-solid PCM and its incorporation in a gypsum paste was studied at 0.5 %, 1 % and 2 % of the weight of the cementitious agent with the aim of developing a material with the capacity to store/release heat through a rapid response to external temperature changes, depending on the percentage of NH addition.

ISSN: 2523-2428

The influence of NH on hydration kinetics and hydrated products, water resistance and physical-mechanical performance, which are indispensable properties in materials used in construction, was also determined.

Experimental Methodology

Starting materials

This study considers the following materials:

1. MAXIMO brand plaster
2. Vanadium Dioxide (VO2) with 99 % purity Alfa AesarTM brand.
3. Multiwalled carbon nanotubes (MWCNT) functionalised with OH radicals of 20-30 nm in diameter and 10 to 30 micrometres in length with 95 % purity brand US Research Nanomaterials Inc.
4. Isopropyl alcohol with 99 % purity CTR Scientific brand.
5. CTR Scientific brand ethylene glycol RA (C2H6O2) dispersant additive (AD) with 99.91 % purity.
6. Potable wáter

NH VO2/MWCNT Synthesis

The preparation of NH was carried out by wet impregnation of MWCNTs and VO2 particles in a ratio of 5/95 wt%.

For this process, the materials (VO2 and MWCNT) were placed in the above mentioned ratio in a beaker and 100 mL of isopropyl alcohol was added for each gram of powder. Afterwards, ultrasound was applied to the solution for 1 hour. Subsequently, NH was obtained by evaporating the isopropanol at 90 °C with constant magnetic stirring until total evaporation of the alcohol. Finally, the powder obtained was heated at 150 °C for 3 hours in order to remove any organic residue from the alcohol.

Preparation of the gypsum pastes

Three mixtures were prepared with NH VO2/MWCNT incorporation of 0.5 %, 1 % and 2 % by weight of the gypsum and a base test tube without addition. Table 1 shows the weight per cubic metre of material for each case.

Mix	Plaster (kg/m^3)	Water (kg/m^3)	NH (kg/m^3)	AD (kg/m^3)
Y0	943.58	589.74	0	0
Y05	943.58	579.92	4.71	9.81
Y1	943.58	579.92	9.43	9.81
Y2	943.58	579.92	18.87	9.81

Table 1 Dosage of the pastes under study

The elaboration of the pastes started withthe dispersion of NH in the mixing water in order to mitigate the agglomeration of the nanocomposite in the matrix (Silvestro & Jean Paul Gleize, 2020). For this, the corresponding amount of VO2/MWCNT and mixing water, the latter consisting of 1 %v AD and 99 %v drinking water, was placed in a vessel. The solution was then subjected to ultrasound for 1 hour. At the end of this process, the resulting solution was mixed with the gypsum following the procedure indicated in ASTM C 305.

The pastes were cast in cylindrical moulds of 2.5 cm diameter x 5 cm height and in cubic moulds of 5 cm per side. Finally, all specimens were demoulded after 24 hours and used once they reached 7 days of age.

Microstructural characterisation

The quantification of the compounds present in the starting materials was carried out by X-ray fluorescence (XRF) on a PANalytical Epsilon3-XL spectrometer using 40 mm diameter and 4 mm thick pellets. The crystalline phases present were determined by X-ray diffraction (XRD) on a PANalytical Empyrean diffractometer in a 2θ range from 10° to 60° with an increment of 0.05° and a scanning speed of 5°/min using copper Kα radiation; the identification of the compounds was carried out using the International Centre for Diffraction Data (ICDD) database. In addition, the weight percentage of the identified phases was quantified using the X'Pert HighScore Plus software.

The morphology of the samples and the NH distribution in the gypsum matrix was observed by scanning electron microscopy (SEM) on a JEOL JSM-6510LV microscope, using a gold-palladium coating on the samples. The wettability of the samples was determined by the water contact angle technique on a Krüss model DSA25E using cubic specimens dried to constant weight at a temperature of 45 °C ± 5°.

ISSN: 2523-2428

Compressive strength

The compressive strength test was performed in accordance with ASTM C 472. Three cylindrical specimens of each percentage of NH addition were used 7 days after preparation. They were then subjected to uniaxial compressive loading until fracture in an Instron model 600DX hydraulic press. A loading rate of 40 psi/s was applied. The results obtained and standard deviation are presented as an average for each sample.

Water resistance

The moisture-drying method was used, which was adapted to the type of material under analysis based on UNE 22190-2 1990 and ASTM D 4843. Three cylindrical samples of each mixture were used and dried to constant weight at a temperature of 45 °C ± 5°. This method began with the total immersion of each specimen in 100 ml of distilled water for 6 hours in a cylindrical glass flask measuring 5 cm in diameter by 12 cm in height, making sure that the sample did not touch the bottom. They were then removed from the water and dried in an oven at 45 °C ± 5° for 12 hours.

This process was carried out in a total of 6 cycles in which the dry and water saturated weights of the specimens were recorded. The total mass loss and water absorption per cycle were calculated with equation 1 and 2, respectively.

$$\%P_m = \frac{P_{i\,s} - P_{6\,s}}{P_{i\,s}} * 100 \quad (1)$$

Where:

$\%P_m$= total mass loss (%), $P_{i\,s}$= initial dry weight of the sample (g) and $P_{6\,s}$= weight of the dry specimen after the 6th cycle (g).

$$\%ABS_x = \frac{P_{saturadoxs} - P_{i\,s\,x}}{P_{i\,s\,x}} * 100 \quad (2)$$

Where:
$\%ABS_x$= water absorption (%) for a given cycle, $P_{saturado\ xs}$= weight of the water-saturated and surface-dried specimen from the post-calculation cycle (g) and $P_{i\,s\,x}$= weight of the dry sample of the cycle under calculation.

The results were then averaged and their standard deviation calculated.

At the end of the 6th cycle, the compressive strength of the specimens was determined in order to evaluate the effect of mass loss on this property.

Thermal properties

The thermal storage capacity and transition temperature of NH was measured by differential scanning calorimetry (DSC) with a TA Instruments model SDTQ600 calorimeter in the temperature range of 30 °C to 100 °C with a heating rate of 2 °C/min in nitrogen atmosphere. The thermal conductivity of the gypsum specimens was measured with a METER model TEMPOS conductivity meter using the SH-3 sensor. Isothermal calorimetry was used to determine the heat of hydration and specific heat in a Calmetrix calorimeter model I-Cal 4000 HPC. The measurement of specific heat was carried out based on that reported by V.-P. Lehto *et al*. (V.-P. Lehto, 1998).

For this purpose, pellets of 25 mm diameter by 10 mm high, without moisture and of known weight were used. They were heated in the temperature range of 25 °C to 55 °C for 1 h. The temperature of the pellet was checked at the temperature range of 25 °C to 55 °C. The temperature of the tablet was checked using a FLIR infrared thermometer model TG165 with an emissivity of 0.80. Immediately afterwards, the pellet was placed inside the calorimeter to start measuring the heat flux released until a temperature of 23 °C was reached (approx. 1 h). Then, the area under the curve of the heat flow graph (Watts) versus time (s) was calculated. The Cp was determined using the following equation.

$$Cp = \frac{Ac}{(T_i - T_c)P_{ms}} \quad (3)$$

Where:
Cp=specific heat (J/kg°C), Ac=area under the curve of the calorimeter measurement (Joules), T_i= initial sample temperature (°C), T_c= calorimeter temperature (°C) (for this experiment was 23 °C) and P_{ms}= weight of dry sample (Kg).

Heating was carried out at 25 °C, 30 °C, 35 °C, 40 °C, 45 °C, 50 °C and 55 °C with 3 measurements for each temperature for each specimen. The Cp obtained were plotted against temperature and linear regression was applied to generate an average line.

ISSN: 2523-2428

Performance of specimens as thermal regulators

This procedure was developed based on the literature related to the study of PCMs (Du *et al*., 2020; Kuai *et al*., 2021; Mohseni *et al*., 2020). For the experiment, a wooden box in the shape of a quadrangular prism with dimensions of 38 cm per side by 53 cm high, with thermal insulation on its inner sides, was used (figure 1). A 300 watt electric heater was placed inside the box at a distance of 34 cm from the lower inner side of the box. In addition, a cubic specimen of 5 cm per side of each mixture was made, trying to introduce a thermocouple in the centre of it, in order to monitor the internal temperature of the specimens with the help of a Perfect Prime TC0309 4-channel thermometer. First, the empty box was heated and once the temperature remained constant at 40 °C ± 5°, the specimens, which were at room temperature (approx. 25 °C), were introduced. Afterwards, the heating temperatures were recorded for 2 hours followed by 3 hours of cooling to room temperatura.

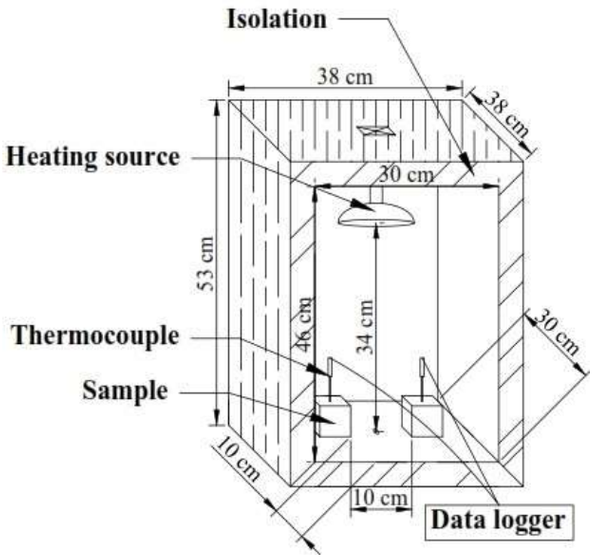

Figure 1 Experimental box arrangement for the evaluation of the thermal performance of pastes

Results

Characterisation of starting materials

The chemical composition of MAXIMO brand gypsum is shown in table 2 below. It details the percentages by weight of the oxides present in this material.

Compound	MAXIMO Gypsum (%p)
SO_3	65.19
CaO	32.34
SiO_2	1.46
Al_2O_3	0.35
K_2O	0.17
MgO	0.16

Table 2 Chemical composition of MAXIMO brand gypsum

Graph 1 illustrates the diffractogram for MAXIMO gypsum, which matched the phase of calcium sulphate hemihydrate or bassanite (CaSO4-½H2O) with Powder Diffraction File (PDF) No.:00-033-0310 and the compound calcium carbonate (CaCO3) or calcite with PDF No.: 01-076-2713. Furthermore, phase quantification indicated 96% bassanite and 4% calcite (table 3). These compounds belong to the expected composition for this type of material (Castellón *et al*., 2021; Rehhoff *et al*., 1990).

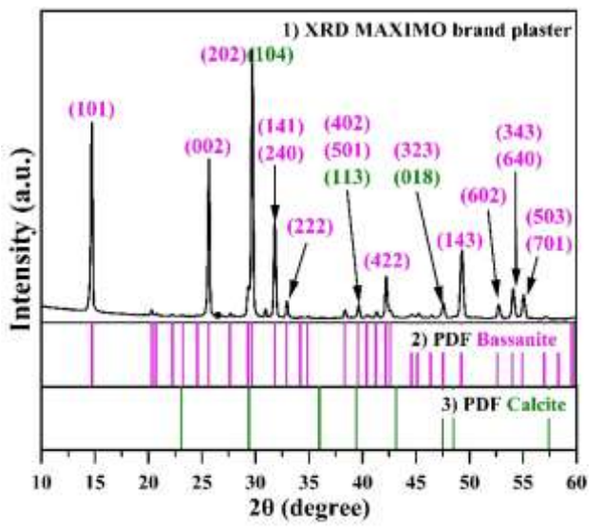

Graph 1 Diffractograms of: 1) XRD of MAXIMO gypsum, 2) PDF of bassanite and 3) PDF of calcite

Compound	%p
Bassanita ($CaSO_4$•½H_2O)	96
Calcite ($CaCO_3$)	4

Table 3 Quantification of MAXIMO® brand gypsum phases

On the other hand, the VO2 diffractogram (graph 2) exhibited congruence with the phase of vanadium dioxide with monoclinic crystalline structure (VO2(M)) with PDF No.: 00-009-0142. This ensures the presence of the compound with phase change properties (Li *et al*., 2017).

ISSN: 2523-2428

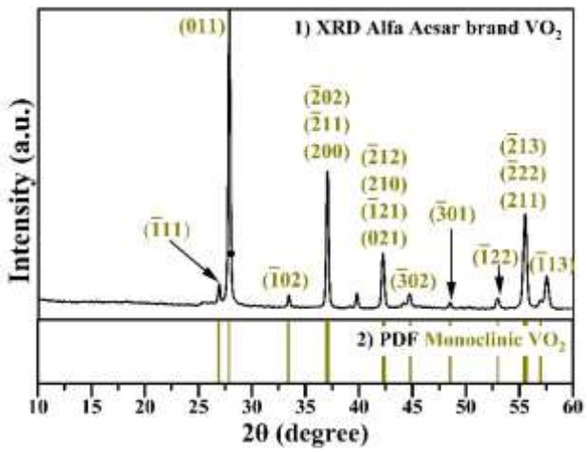

Graph 2 Diffractogram of: 1) XRD of Alpha Aesar brand VO2 and 2) PDF of VO2 with monoclinic crystal structure

Finally, graph 3 shows the result of the XRD analysis of MWCNTs, where the identified phase corresponds to carbon with hexagonal crystalline structure according to PDF No.:00-001-0640.

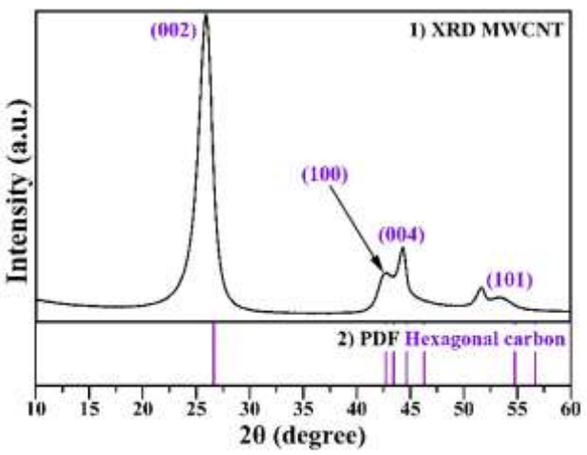

Graph 3 Diffractogram of: 1) XRD of MWCNTs and 2) PDF of carbon with hexagonal crystal structure

Characterisation of NH VO2/MWCNT

Once the NH was synthesised, the DSC technique was used on pure VO2 and NH VO2/MWCNT in order to obtain the heat flux graphs shown in graph 4.

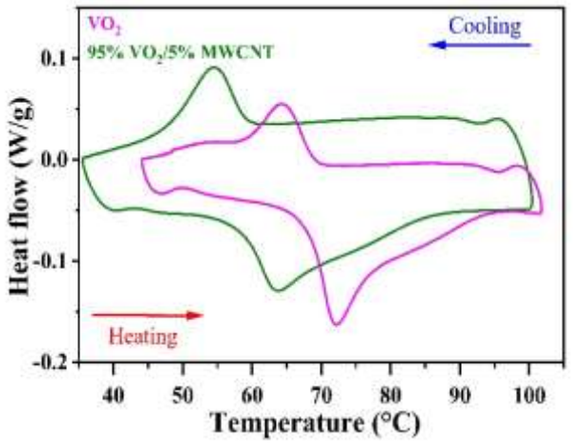

Graph 4 Heat flow diagram of pure VO2 and NH 95%VO2/5%MWCNT

The estimates resulted in a heating and cooling Tc of 72.41 ± 0.37 °C and 64.15 ± 0.16 °C for VO2 and 63.73 ± 0.59 °C and 54.53 ± 0.12 °C for VO2/MWCNT. The reduction in Tc is attributed to the presence of MWCNTs in the NH, which increases the thermal conductivity resulting in the improvement of the absorption/release dynamics of the PCM. In addition, a latent heat of heating and cooling of 40.51 ± 0.41 J/g and 22.84 ± 1.14 J/g in VO2 and 32.06 ± 0.53 J/g and 19.35 ± 0.84 J/g for NH were obtained. This reduction in latent heat of NH is caused by the integration of MWCNTs in NH due to the decrease in the amount of VO2 available to store heat.

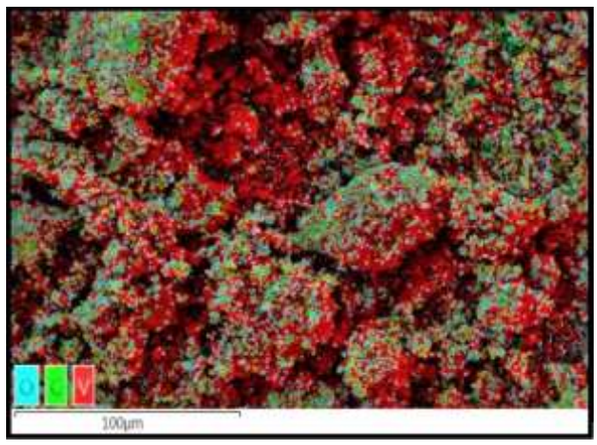

Figure 2 EDS analysis of NH VO2/MWCNT with a focus on the elements oxygen, carbon and vanadium

Sic., figure 2 illustrates the energy dispersive spectroscopy (EDS) analysis of NH. The scattering of MWCNTs on the VO2 surface is observed, which exhibits the saturation of the PCM particles with the thermal conductivity enhancer.

ISSN: 2523-2428

Microstructural characterisation

With the XRD analysis of the hardened pastes, the diffractograms shown in graph 5 were obtained. Firstly, a development of hydration phases is observed with the presence of calcium sulphate dihydrate or gypsum (CaSO4-2H2O) with PDF No.: 00-003-0044, calcite and bassanite (CaSO4-2H2O) with PDF No.: 00-003-0044, calcite and bassanite.

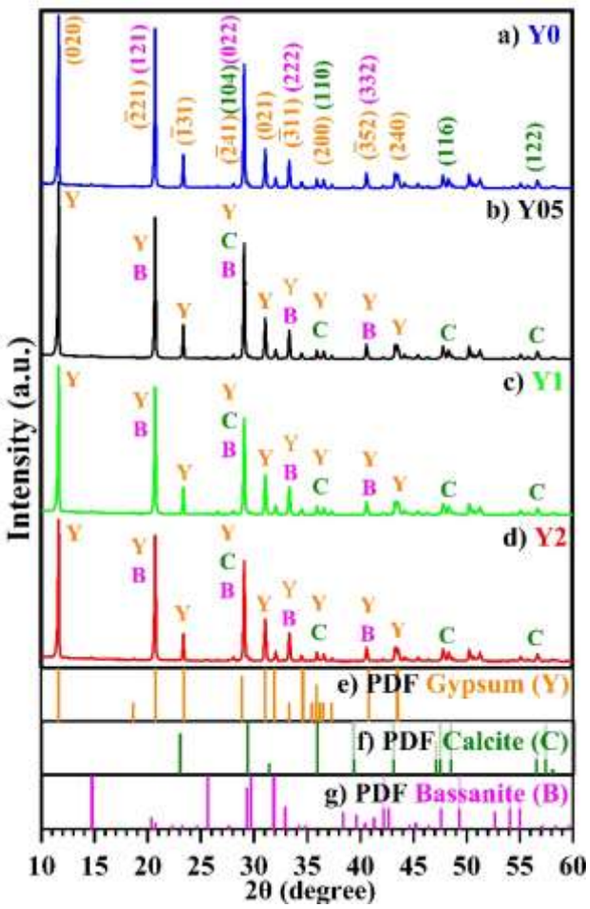

Graph 5 Diffractograms of 7-day-old pastes of: a) Y0, b) Y05, c) Y1, d) Y2, e) gypsum PDF, f) calcite PDF and g) bassanite PDF

In addition to this, phase quantification (table 4) indicates a similar development of the gypsum phase for all samples, however, samples Y1 and Y2 showed 2 % and 4 % of the bassanite phase. Despite this, the diffractograms of the samples show no change in phase development between them.

Compound	Y0 (%p)	Y05 (%p)	Y1 (%p)	Y2 (%p)
Plaster	97	98	98	96
Calcite	3	2	-	-
Bassanita	-	-	2	4

Table 4 Phase quantification of samples Y0, Y05, Y1 and Y2 at 7 days of age

The analysis of the morphology of the matrices (figure 3) showed that the samples consist of particles of similar size in all cases, with the presence of elongated gypsum crystals with lengths of 8-10 microns and widths of 1-5 microns (Vimmrová *et al*., 2020). This is related to the similar phase development illustrated in the XRD analysis of the pastes (graph 5).

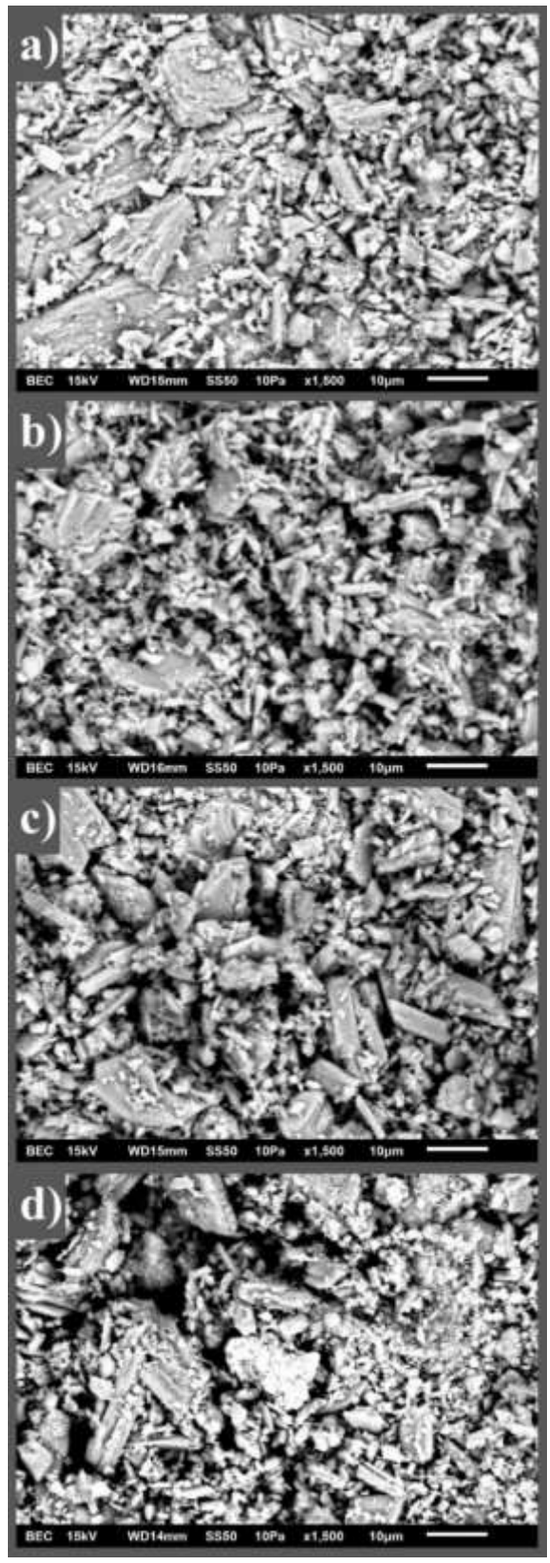

Figure 3 Microscopies at 1500 magnification of: a) Y0, b) Y05, c) Y1 and d) Y2

ISSN: 2523-2428

Compressive strength

The compressive strength is presented in graph 6. Here, all the specimens presented a similar strength value of 6.71 Mpa. This indicates that the integration of NH in the gypsum matrix does not generate any modification in the compressive strength development of the pastes with respect to a mix without addition at 7 days of age.

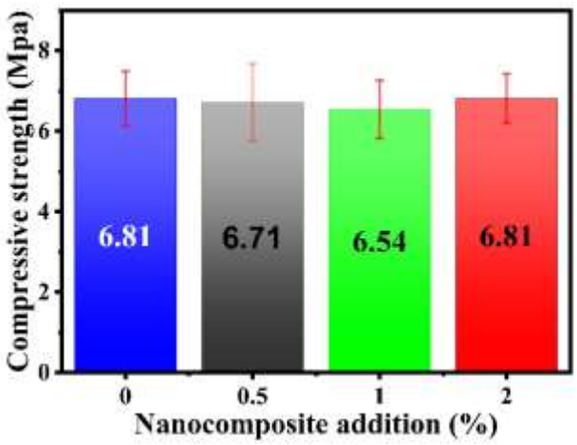

Graph 6 Compressive strength of gypsum pastes

Hydration kinetics

The isothermal calorimetry resulted in the graphs shown in graph 7. The same behaviour of heat release with respect to time due to the exothermic hydration reaction of commercial gypsum is observed for all the samples.

It is interpreted that the presence of NH in the gypsum matrix does not modify the heat flux released during hydration. On the other hand, after 24 hours the total accumulated heat remains similar for all cases. This reveals that NH does not generate alterations in the hydration kinetics of the mixtures or in the development of the hydrated products, which correlates with the diffractograms in graph 5.

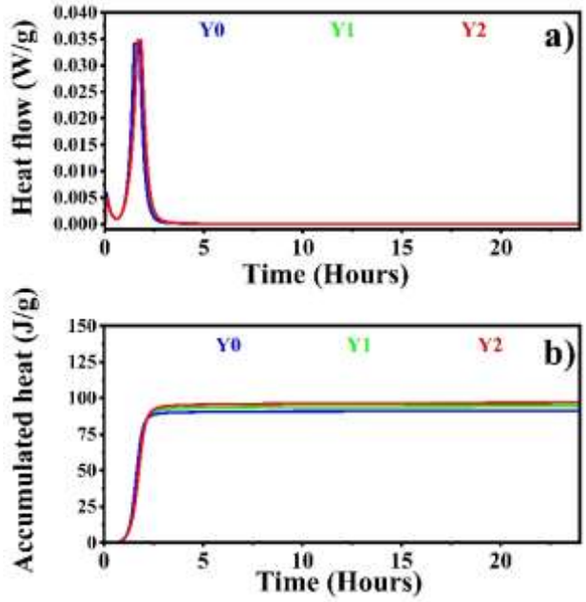

Graph 7 Isothermal calorimetry of the pastes. a) graph of the heat flow released and b) graph of the accumulated heat released

Wettability of simples

The water contact angle is an indicator of the surface permeability of materials (Jin *et al.*, 2021). Figure 4 shows the resulting angles measured by this technique. It can be seen that the contact angle value is similar for the four samples presenting a value around 65 ° indicating that the samples are hydrophilic (Gomes *et al.*, 2013) and that the integration of NH in the gypsum matrix did not have a direct effect on the wettability of the material.

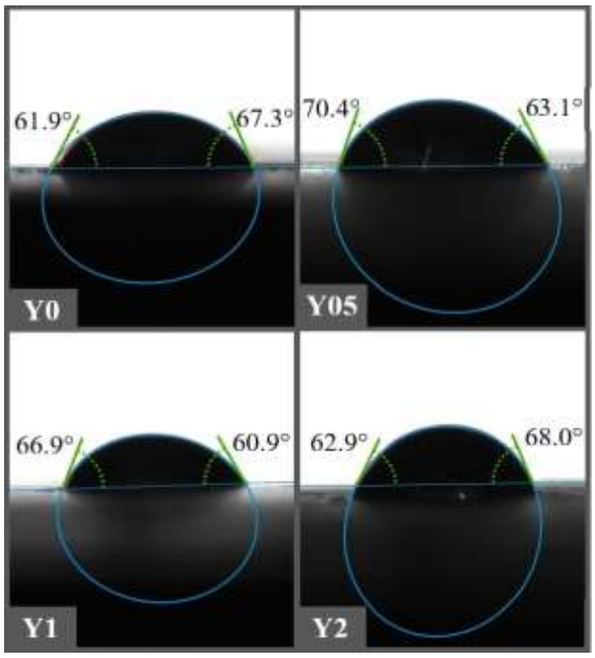

Figure 4 Water contact angle of gypsum pastes

ISSN: 2523-2428

Water resistance

Graph 8 illustrates the percentage mass loss for each specimen after 6 moisture-drying cycles and their compressive strength at the end of the process. Where, the specimens reduced their mass by 2.96 %, 3.23 %, 3.52 % and 3.4 % for Y0, Y05, Y1 and Y2 respectively. Therefore, the incorporation of NH into the gypsum paste increases the dissolution of the material in an aqueous medium, increasing the mass loss by 9.12 %, 18.91 % and 14.86 % when integrating 0.5 %, 1 % and 2 % VO2/MWCNT with respect to the gypsum without NH. In addition, a trend of increasing mass loss is observed between Y0, Y05, Y1, however, Y2 improved this capacity by decreasing the percentage of mass loss by 4.05 % compared to Y1.

Also, graph 8 shows the compressive strength values of the specimens after 6 cycles. Where, specimen Y0 exhibited a strength of 6.55 Mpa which is similar to that obtained at 7 days of age, so its mechanical performance was not affected by the loss of mass. On the other hand, Y05, Y1 and Y2 showed a compressive strength of 9.42 Mpa, 9.97 Mpa and 8.02 Mpa, respectively.

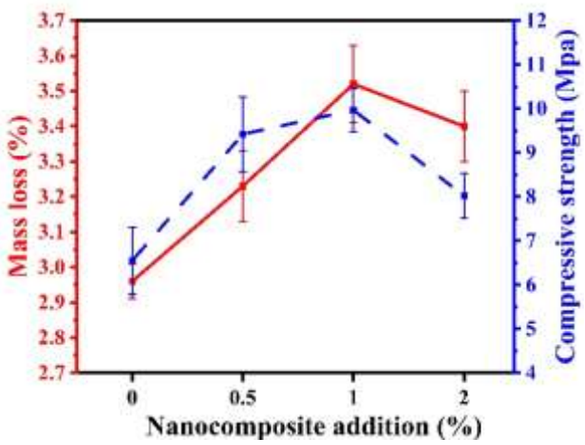

Graph 8 Percentage mass loss and compressive strength after 6 wetting-drying cycles of gypsum pastes

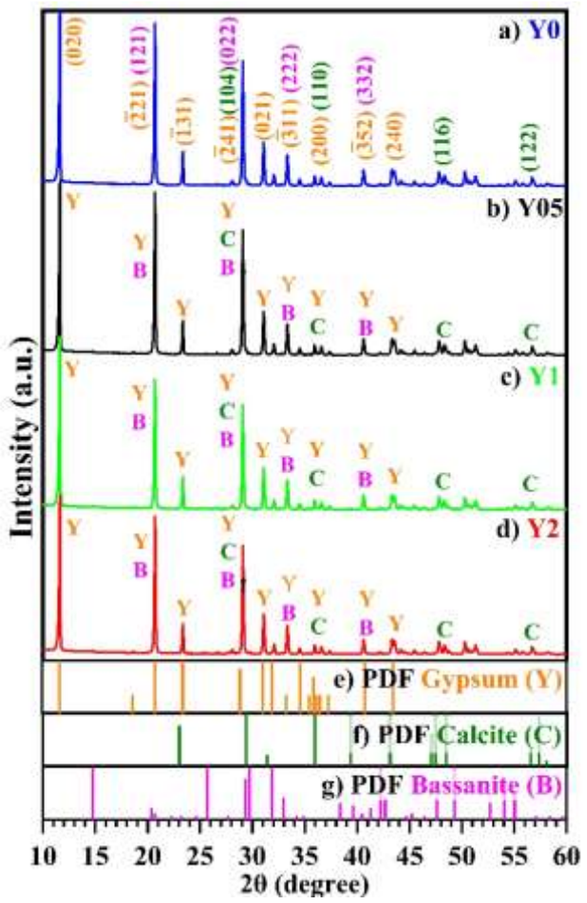

Graph 9 Diffractograms obtained after 6 wetting-drying cycles of: a) Y0, b) Y05, c) Y1, d) Y2, e) gypsum PDF, f) calcite PDF and g) bassanite PDF

Compound	Y0 (%p)	Y05 (%p)	Y1 (%p)	Y2 (%p)
Plaster	96	100	100	97
Calcite	3	-	-	-
Bassanita	1	-	-	3

Table 5 Phase quantification of Y0, Y05, Y1 and Y2 after 6 cycles of the humidity-drying method

Graph 9 shows the diffractograms corresponding to the pastes with and without NH addition after the wetting-drying cycles. It shows similar phases to those exhibited in the samples at 7 days of age, however, the quantification of the phases (table 5) revealed an increase in the amount of gypsum and a decrease in the bassanite phase, which explains the increase in compressive strength of the pastes shown in graph 8.

Graph 10 shows the percentages of water absorption for each sample during the cycles of the moisture-drying method. The reduction in absorption of samples Y05, Y1 and Y2 with respect to sample Y0 is observed. This indicates that NH decreases the absorption of the gypsum pastes.

ISSN: 2523-2428

This is attributable to the formation of denser matrices compared to a mixture without addition, since NH occupies voids in the gypsum microstructure.

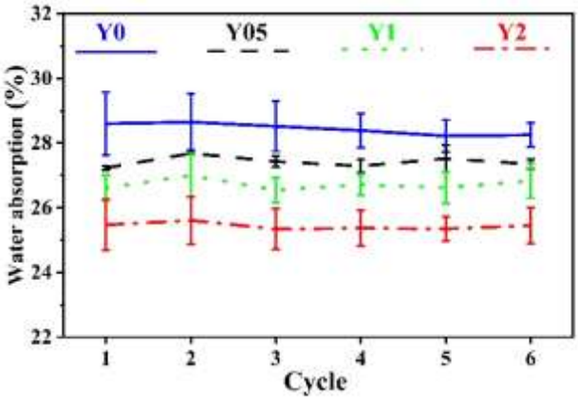

Gráfica 10 Percentage of water absorption in each wetting-drying cycle of gypsum pastes

Thermal properties

The analysis of the thermal behaviour started with the determination of the thermal conductivity of the specimens. Table 6 reports the values obtained for each sample. The integration of NH in the pastes increases the thermal conductivity value by 0.47 %, 1.07 % and 1.43 % with the addition of 0.5 %, 1 % and 2 % of NH VO2/MWCNT, respectively. The increase of this property is caused by the presence of NH in the cementitious matrix due to 2 reasons: 1. Because of the thermal conductivity of VO2, which is reported to be higher than that of gypsum (Barra *et al*., 2021) and 2.

Sample	Thermal conductivity (W/mK)
Y0	0.4184 ± 0.01
Y05	0.4204 ± 0.009
Y1	0.4229 ± 0.0069
Y2	0.4244 ± 0.01

Table 6 Thermal conductivity of samples

Graph 11 shows the specific heat of the specimens within the range of 25 °C to 55 °C. The interpretation of the diagram shows that at 25.8 °C the Cp of samples Y05, Y1 and Y2 increased by 0.5 %, 1.2 %, and 1.5 %, with respect to the sample without additions. Furthermore, as the temperature increases up to 55°C the Cp of samples Y0, Y05 and Y1 slightly decreased, while Y2 gradually increased its value.

From this it can be stated that at 55°C the Cp of samples Y05, Y1 and Y2 increased their Cp by 0.95 %, 1.91 % and 4.85 % with respect to Y0. This phenomenon is attributed to the heat storage of NH in the pastes. Since, when heat flows through the paste, the PCM particles closest to the heat source are energetically equilibrated before the subsequent ones until all the particles in the system equalise in temperature. Due to this phenomenon, the Cp of NH pastes increases in value as the temperature increases.

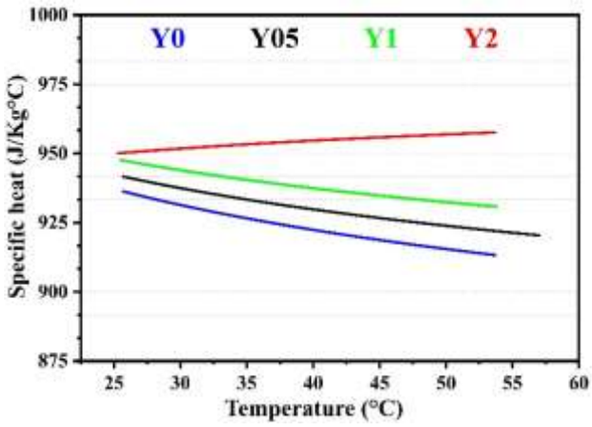

Graph 11 Specific heat of pastes with and without addition of NH

Performance of pastes as thermal regulators

The results of the analysis of the thermal behaviour of the specimens when the outside temperature is 40 °C and their cooling to room temperature (25 °C) are shown in graph 12. It compares the temperature increase as a function of time of the specimens with and without NH. It can be observed that, during heating, the increase in the internal temperature of the samples with NH incorporation remained below the Y0 sample, i.e., in the pure gypsum it took 1 h 40 min 17 s to reach 40 °C, whereas, the materials with the addition of 0.5 %, 1 % and 2 % of NH took 1 h 41 min 11 s, 1 h 44 min 24 s and 2 hours 2 min 20 s, respectively. Comparing the temperature of the samples with NH at the same time as the pure gypsum reached 40 °C, the samples with NH showed a temperature differential of 0.1 °C, 1.1 °C and 0.8 °C, respectively.

The higher the amount of NH added, the longer the time for the temperature of the samples to reach 40 °C, indicating that the gypsum with NH is storing heat.

ISSN: 2523-2428

Conversely, during cooling, specimen Y0 decreased its temperature at a faster rate compared to the NH-incorporated samples. Pure gypsum took 1 h 25 min 57 s to reach 25 °C, while the time for Y05, Y1 and Y2 was 1 h 33 min 16 s, 1 h 50 min 33 s and 2 h 40 min 17 s, respectively. When comparing the temperature of gypsum with NH at the same time as pure gypsum reached 25 °C, a temperature differential of 0.2 °C, 0.5 °C and 0.5 °C, respectively, was observed.

This phenomenon occurs due to the increase in the Cp of the samples with NH, as observed in graph 11. This can be attributed to the fact that the higher the amount of NH, the higher the amount of heat stored. The variations in the heating and cooling times of pure gypsum indicate that the gypsum with NH acts as a thermal regulator in both increasing and decreasing the external temperature, which would contribute to maintaining thermal comfort and consequently to the energy efficiency of a building.

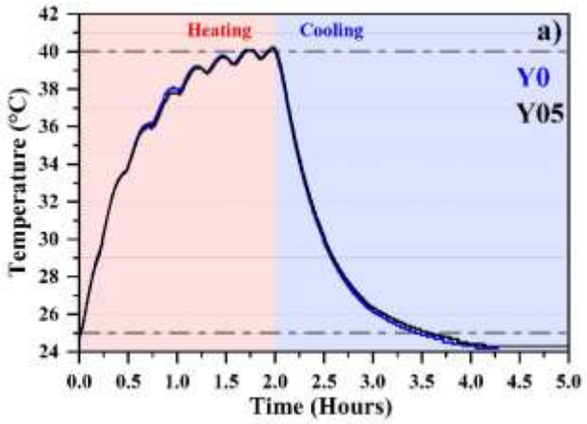

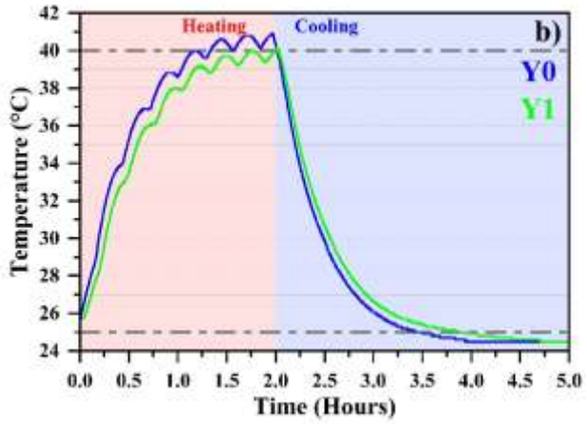

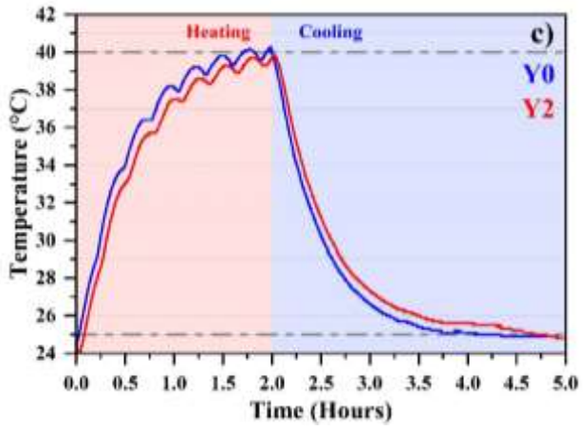

Graph 12 Thermal behaviour of gypsum pastes at 40 °C. a) Y0 vs Y05, b) Y0 vs Y1, and c) Y0 vs Y2

Acknowledgement

Thanks are extended to the Universidad Autónoma de Nuevo León, specifically to the Centro de Investigación e Innovación de Materiales de Construcción of the Facultad de Ingeniería Civil which provided the equipment, personnel and furniture to carry out the research presented here.

Funding

This work has been funded by the Programa de Apoyo a la Investigación Científica y Tecnología de la UANL, PACYT [559-IT-2022 and 608-CAT-2022]; CONACYT [master's grant No. 1106862].

Conclusions

This paper presented the preparation and incorporation of a NH of VO2/MWCNT in gypsum pastes, the corresponding additions were 0.5 %, 1 % and 2 % in relation to the weight of the cementitious agent. The results obtained showed that there is a good compatibility and homogeneous integration between gypsum and NH as the development of the hydrated compounds and the values of compressive strength, wettability and water resistance were not affected. It was found that the addition of NH had a significant effect on the thermal properties of the gypsum with an increase in thermal conductivity by 1.43 % compared to pure gypsum. The Cp value also showed an increase in its estimates.

ISSN: 2523-2428

This influenced the heating/cooling rate of the samples with NH giving the gypsum the ability to store heat during external temperature rises and release it when the external temperature drops by acting as a thermal regulator, which makes it attractive for the preparation of energy efficient building materials.

References

Alzoubi, H. H., Albiss, B. A., & Abu sini, S. S. (2020). Performance of cementitious composites with nano PCMs and cellulose nano fibers. *Construction and Building Materials*, *236*. https://doi.org/10.1016/j.conbuildmat.2019.117483

Amaral, C., Vicente, R., Marques, P. A. A. P., & Barros-Timmons, A. (2017). Phase change materials and carbon nanostructures for thermal energy storage: A literature review. *Renewable and Sustainable Energy Reviews*, *79*(January), 1212–1228. https://doi.org/10.1016/j.rser.2017.05.093

Barra, H. M., Chen, S. K., Tamchek, N., Talib, Z. A., Lee, O. J., & Tan, K. B. (2021). Phase, Microstructure, Thermochromic, and Thermophysical Analyses of Hydrothermally Synthesized W-Doped VO2Nanopowder. *Advances in Materials Science and Engineering*, *2021*. https://doi.org/10.1155/2021/8582274

Boccarusso, L., Durante, M., Iucolano, F., Langella, A., Minutolo, F. M. C., & Mocerino, D. (2020). Recyclability process of standard and foamed gypsum. *Procedia Manufacturing*, *47*(2019), 743–748. https://doi.org/10.1016/j.promfg.2020.04.227

bp report. (2022). Statistical Review of World Energy 2022. Recuperado el 8 de septiembre del 2022 de https://www.bp.com/content/dam/bp/business-sites/en/global/corporate/pdfs/energy-economics/statistical-review/bp-stats-review-2022-full-report.pdf

Castellón, F. J., Ayala, M., Flores, J. A., & Lanzón, M. (2021). Influence of citric acid on the fire behavior of gypsum coatings of construction and structural elements. *Materiales de Construccion*, *71*(341). https://doi.org/10.3989/MC.2021.13120

Cheng, T., Wang, N., Wang, H., Sun, R., & Wong, C. P. (2020). A newly designed paraffin@VO2 phase change material with the combination of high latent heat and large thermal conductivity. *Journal of Colloid and Interface Science*, *559*, 226–235. https://doi.org/10.1016/j.jcis.2019.10.033

Coppola, L., Coffetti, D., & Lorenzi, S. (2016). Cement-Based Renders Manufactured with Phase-Change Materials: Applications and Feasibility. *Advances in Materials Science and Engineering*, *2016*. https://doi.org/10.1155/2016/7254823

Cunha, S., Silva, M., & Aguiar, J. (2020). Behavior of cementitious mortars with direct incorporation of non-encapsulated phase change material after severe temperature exposure. *Construction and Building Materials*, *230*, 117011. https://doi.org/10.1016/j.conbuildmat.2019.117011

Du, Y., Liu, P., Quan, X., & Ma, C. (2020). Characterization and cooling effect of a novel cement-based composite phase change material. *Solar Energy*, *208*(July), 573–582. https://doi.org/10.1016/j.solener.2020.07.083

Fallahi, A., Guldentops, G., Tao, M., Granados-Focil, S., & van Dessel, S. (2017). Review on solid-solid phase change materials for thermal energy storage: Molecular structure and thermal properties. *Applied Thermal Engineering*, *127*, 1427–1441. https://doi.org/10.1016/j.applthermaleng.2017.08.161

Faraj, K., Khaled, M., Faraj, J., Hachem, F., & Castelain, C. (2020). Phase change material thermal energy storage systems for cooling applications in buildings: A review. *Renewable and Sustainable Energy Reviews*, *119*(May 2019), 109579. https://doi.org/10.1016/j.rser.2019.109579

Frazzica, A., Brancato, V., Palomba, V., la Rosa, D., Grungo, F., Calabrese, L., & Proverbio, E. (2019). Thermal performance of hybrid cement mortar-PCMs for warm climates application. *Solar Energy Materials and Solar Cells*, *193*(January), 270–280. https://doi.org/10.1016/j.solmat.2019.01.022

ISSN: 2523-2428

Gomes, D. J. C., de Souza, N. C., & Silva, J. R. (2013). Using a monocular optical microscope to assemble a wetting contact angle analyser. *Measurement: Journal of the International Measurement Confederation*, *46*(9), 3623–3627. https://doi.org/10.1016/j.measurement.2013.07.010

Guardia, C., Barluenga, G., Palomar, I., & Diarce, G. (2019). Thermal enhanced cement-lime mortars with phase change materials (PCM), lightweight aggregate and cellulose fibers. *Construction and Building Materials*, *221*, 586–594. https://doi.org/10.1016/j.conbuildmat.2019.06.098

Jeong, S. G., Wi, S., Chang, S. J., Lee, J., & Kim, S. (2019). An experimental study on applying organic PCMs to gypsum-cement board for improving thermal performance of buildings in different climates. *Energy and Buildings*, *190*, 183–194. https://doi.org/10.1016/j.enbuild.2019.02.037

Jin, Z., Ma, B., Su, Y., Qi, H., Lu, W., & zhang, T. (2021). Preparation of eco-friendly lightweight gypsum: Use of beta-hemihydrate phosphogypsum and expanded polystyrene particles. *Construction and Building Materials*, *297*. https://doi.org/10.1016/j.conbuildmat.2021.123837

Kim, Y. U., Park, J. H., Yun, B. Y., Yang, S., Wi, S., & Kim, S. (2021). Mechanical and thermal properties of artificial stone finishing materials mixed with PCM impregnated lightweight aggregate and carbon material. *Construction and Building Materials*, *272*, 121882. https://doi.org/10.1016/j.conbuildmat.2020.121882

Kuai, C., Chen, J., Shi, X., & Grasley, Z. (2021). Regulating porous asphalt concrete temperature using PEG/SiO2 phase change composite: Experiment and simulation. *Construction and Building Materials*, *273*, 122043. https://doi.org/10.1016/j.conbuildmat.2020.122043

Li, M., Magdassi, S., Gao, Y., & Long, Y. (2017). Hydrothermal Synthesis of VO2 Polymorphs: Advantages, Challenges and Prospects for the Application of Energy Efficient Smart Windows. *Small*, *13*(36), 1–25. https://doi.org/10.1002/smll.201701147

Lushnikova, N., & Dvorkin, L. (2016). Sustainability of gypsum products as a construction material. In *Sustainability of Construction Materials* (Second Edi). Elsevier Ltd. https://doi.org/10.1016/b978-0-08-100370-1.00025-1

Mohseni, E., Tang, W., Khayat, K. H., & Cui, H. (2020). Thermal performance and corrosion resistance of structural-functional concrete made with inorganic PCM. *Construction and Building Materials*, *249*, 118768. https://doi.org/10.1016/j.conbuildmat.2020.118768

Raj, C. R., Suresh, • S, Bhavsar, • R R, Vivek, •, Singh, K., Bhavsar, R. R., & Singh, V. K. (2020). Recent developments in thermo-physical property enhancement and applications of solid solid phase change materials A review. *Journal of Thermal Analysis and Calorimetry*, *139*, 3023–3049. https://doi.org/10.1007/s10973-019-08703-w

Rehhoff, L., Akkermans, P. M. M. G., Leonardsen, E., & Thuesen, I. (1990). Plasters : Gypsum or Calcite ? A Preliminary Case Study of Syrian Plasters. *Paléorient*, *16*(2), 79–87. https://doi.org/10.3406/paleo.1990.4534

Silvestro, L., & Jean Paul Gleize, P. (2020). Effect of carbon nanotubes on compressive, flexural and tensile strengths of Portland cement-based materials: A systematic literature review. *Construction and Building Materials*, *264*, 120237. https://doi.org/10.1016/j.conbuildmat.2020.120237

Tyagi, V. V., & Buddhi, D. (2007). PCM thermal storage in buildings: A state of art. *Renewable and Sustainable Energy Reviews*, *11*(6), 1146–1166. https://doi.org/10.1016/j.rser.2005.10.002

ISSN: 2523-2428

Vimmrová, A., Krejsová, · J, Scheinherrová, · L, Doleželová, · M, & Keppert, · M. (2020). Changes in structure and composition of gypsum paste at elevated temperatures. *Journal of Thermal Analysis and Calorimetry*, *142*, 19–28. https://doi.org/10.1007/s10973-020-09528-8

V.-P- Lehto, M. R. E. Laine. L. Y. P. H. and K. J. (1998). Determination of specific heats using isothermal microcalorimetry. *Journal of Thermal Analysis*. https://doi.org/https://doi.org/10.1002/jbm.b.10044

Yu, S., Jeong, S. G., Chung, O., & Kim, S. (2014). Bio-based PCM/carbon nanomaterials composites with enhanced thermal conductivity. *Solar Energy Materials and Solar Cells*, *120*(PART B), 549–554. https://doi.org/10.1016/j.solmat.2013.09.037

Zuo, X., Zhao, X., Li, J., Hu, Y., Yang, H., & Chen, D. (2020). Enhanced thermal conductivity of form-stable composite phase-change materials with graphite hybridizing expanded perlite/paraffin. *Solar Energy*, *209*(July), 85–95. https://doi.org/10.1016/j.solener.2020.08.082

ISSN: 2523-2428